

Original Article

[¹¹C]5-Hydroxy-tryptophan model for quantitative assessment of in vivo serotonin biosynthesis, retention and degradation in the endocrine pancreas

Mark Lubberink¹, Olof Eriksson²

¹Department of Surgical Sciences, Uppsala University, Uppsala, Sweden; ²Science for Life Laboratory, Department of Medicinal Chemistry, Uppsala University, Uppsala, Sweden

Received April 8, 2020; Accepted September 8, 2020; Epub October 15, 2020; Published October 30, 2020

Abstract: [¹¹C]5-Hydroxy-tryptophan ([¹¹C]5-HTP) is a Positron Emission Tomography marker for serotonergic biosynthesis and degradation, with use in imaging of neuroendocrine tumors and recently also the endocrine pancreas in diabetes. In order to further develop [¹¹C]5-HTP as a quantitative in vivo tool for understanding the mechanisms of serotonin signaling in human pancreas, we aimed to develop a kinetic modeling approach sensitive for changes in serotonin biosynthesis, retention and degradation. Cynomolgus monkeys were examined by [¹¹C]5-HTP PET/CT, either at baseline (n=9) or following intravenous pretreatment with 3 mg/kg carbidopa (Dopa Decarboxylase inhibitor, n=3) or 2 mg/kg clorgyline (Monoamine Oxidase-A inhibitor, n=5). The dynamic tissue uptake was analysed by a 2-tissue compartment model including an efflux mechanism from the second tissue compartment (2TC k_{loss}), which theoretically reproduces the known processing of 5-HTP in neuroendocrine cells. The 2TC k_{loss} model could accurately describe all three modes of tissue kinetics depending on the pretreatment regimen. Rate constant k_3 (corresponding to DDC activity) and the macro-parameter Flux (K_i) was decreased ($P < 0.05$) by carbidopa pretreatment, while k_2 (corresponding to cellular washout of intact [¹¹C]5-HTP) was increased ($P < 0.05$). The efflux parameter k_{loss} (corresponding to MAO-A activity) was decreased ($P < 0.05$) by pretreatment of clorgyline, while the macro-parameter Flux/Efflux ratio (K_i/k_{loss}) was increased ($P < 0.0001$). We present a compartment model analysis method that can quantitatively assess in vivo pharmacological interactions with several of the key enzymatic steps of the serotonergic biosynthesis in pancreas.

Keywords: Pancreas, serotonin, islet of langerhans, neuroendocrine, islet mass, beta cell mass

Introduction

Peripheral monoamine signaling has been largely unexplored by means of modern medical imaging technology. Several Positron Emission Tomography (PET) radioligands for visualization of the serotonergic, dopaminergic and noradrenergic systems have been developed but primarily studied in the central nervous system (CNS) [1-3].

Serotonin is perhaps mainly recognized as an important neurotransmitter in the brain, closely linked to mood and depression, but in fact almost 90% the endogenous serotonin reside in the gastrointestinal (GI) tract. The peripheral actions of serotonin are several and include regulation of GI motility, vasoconstriction,

wound healing and more. Recently, it has been shown that serotonin has important actions also in the pancreas; the molecular machinery necessary for serotonin biosynthesis and degradation is present in the beta cells [4], implicated in insulin secretion [5] and linked to beta cell proliferation during pregnancy [6]. Additionally, as the serotonin system is restricted to islets with no expression in the exocrine pancreas [4, 7-10] the radiolabeled serotonin precursor [¹¹C]5-Hydroxy-tryptophan ([¹¹C]5-HTP) has recently been validated as an imaging biomarker for pancreatic islet mass in metabolic disease [11-14].

Figure 1A shows a schematic representation of the metabolic fate of [¹¹C]5-HTP in neuroendocrine cells. [¹¹C]5-HTP enters the neuroendo-

Model of [^{14}C]5-HTP in pancreas

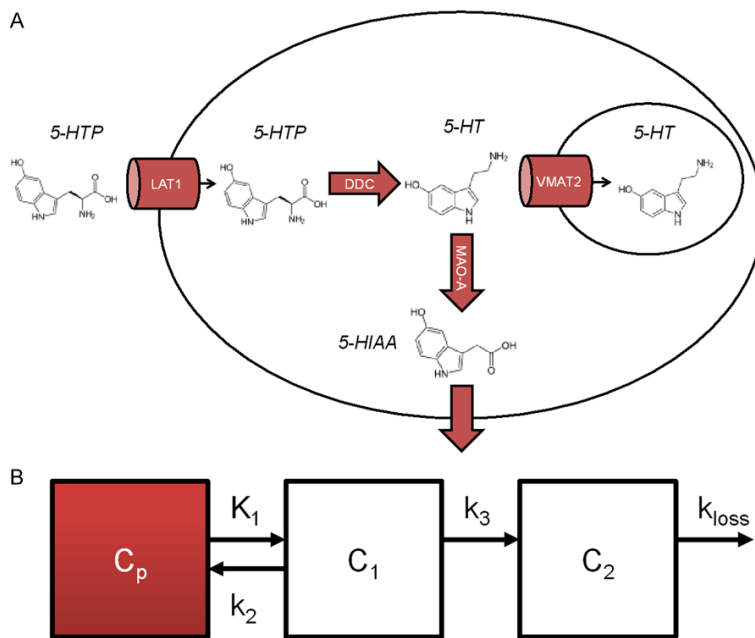


Figure 1. Schematic representation of the major steps in the serotonergic metabolic pathway in neuroendocrine cells (A). A PET compartmental model should be versatile enough to take these processes into account, while still minimizing the amount of parameters to be fitted. The 2-tissue compartment (2TC) model with an efflux (k_{loss}) parameter is a potential model describing the important processes in the neuroendocrine cell (B).

crine cell through Large Amine Transporters (LATs) and is then converted into [^{14}C]5-HT (i.e. ^{14}C -labelled serotonin) by Dopa Carboxylase (DDC, also known as Aromatic L-amino acid decarboxylase). [^{14}C]5-HT may then be transported into intracellular vesicles by the Vesicular Monoamine Transporter 2 (VMAT2). Inside the vesicles, [^{14}C]5-HT is shielded from degradation. The population of [^{14}C]5-HT in the cytosol however, is subject to degradation by Monoamine Oxidase-A (MAO-A) into [^{14}C]5-hydroxyindoleacetic acid ([^{14}C]5-HIAA) which is eliminated across the cell membrane for further urinary excretion.

In the context of the beta cells, the intracellular vesicles also contain insulin, which may be secreted together with 5-HT as a response to changes blood glucose, following exocytosis. VMAT2 has for this reason been extensively evaluated as an imaging marker for visualization of pancreatic beta cells [15, 16].

Previously, an irreversible two tissue compartment (2TC) model has been used as a model for [^{14}C]5-HTP uptake, retention and elimination in the brain [17]. This model assumes that the

degradation by MAO-A is negligible during the first hour after intravenous administration of [^{14}C]5-HTP. However, it has recently been shown that inhibition of MAO-A strongly impacts the in vivo metabolism of [^{14}C]5-HTP [11], indicating that further model development could improve the kinetic PET analysis.

In order to further develop [^{14}C]5-HTP as a quantitative in vivo tool for understanding the mechanisms of serotonin signaling in human pancreas, we here report an optimized compartment model sensitive for changes in serotonin biosynthesis, retention and degradation.

Methods and materials

Study design

The analysis uses dynamic data on [^{14}C]5-HTP uptake in pancreas in non-diabetic non-human primates (NHP). Semi-quantitative analysis (Standardized Uptake Values (SUV) or % of injected dose/g of tissue (%ID/g)) of some of the PET examinations has been reported previously [11].

[^{14}C]5-HTP PET in non-human primates

Imaging protocol, anesthesia, animal handling and tracer metabolite analysis protocol has been reported in detail previously [11]. The animal experiments were approved by the local Animal Research Ethical Committee and were performed according to the Uppsala University guidelines on animal experimentation (UFV 2007/724).

Non-human primates (NHPs, female cynomolgus monkeys, 3-9 kg) were examined by a Discovery ST PET/CT (GE Healthcare) after an intravenous (IV) bolus injection of [^{14}C]5-HTP (5-20 MBq/kg). Carbon-11 has a radioactive half-life of 20 minutes and consequently the signal is fully decayed after approximately 2 h. Then, a second [^{14}C]5-HTP PET examination

Model of [¹¹C]5-HTP in pancreas

Table 1. Metabolic stability of [¹¹C]-5HTP in non-human primates in vivo, at baseline or after pretreatment with carbidopa (DDC inhibitor) or clorgyline (MAO-A inhibitor)

	5 min	30 min	60 min
Baseline (n=7)	90.7±1.5	67.8±2.7	53.5±2.5
DDC inhibited (n=1)	94.8	87.4	79.4
MAO-A inhibited (n=5)	94.3±2.6	77.3±3.8	62.0±4.5

Values indicate percentage of intact [¹¹C]-5HTP as averages and SD.

was performed, this time following IV pretreatment with 3 mg/kg carbidopa or 2 mg/kg clorgyline, in order to inhibit key enzyme steps of the pancreatic serotonin metabolic pathway: DDC or MAO-A respectively. In total, n=9 baseline scans were performed, n=3 scans with DDC inhibited and n=5 scans with MAO-A inhibited.

For all examinations PET data was acquired for 90 minutes (divided into 33 frames; 12×10 s, 6×30 s, 5×120 s, 5×300 s and 5×600 s). Venous blood was collected at 0.5, 1, 3, 5, 10, 15, 20, 30, 45, 60 and 90 minutes to obtain whole blood to plasma ratios.

Due to restriction on blood sampling volume metabolite analysis could only be performed on a subset of NHPs: [¹¹C]5-HTP alone i.e. baseline (n=7), following carbidopa pretreatment (n=1) and following clorgyline pretreatment (n=5). In these animals, the fraction of remaining native [¹¹C]5-HTP was determined in blood samples 5, 30 and 60 minutes following IV administration.

Image analysis

Reconstructed images were analyzed using PMOD 3.7 (PMOD Technologies Ltd., Zurich, Switzerland). Pancreas was segmented pixel-by-pixel with assistance from co-registered CT projections. Only pixels within pancreas, with minimal partial volume effects were included. An image derived input function (IDIF) was obtained by identifying single pixels on transaxial projections fully within vena cava. Maximum Intensity Projection (MIP) images were generated in Carimas 2.9 (Turku PET Center, Turku, Finland).

Pharmacokinetic analysis was performed using standard nonlinear regression techniques using the PKIN module (PMOD Technologies

Ltd., Zurich, Switzerland). A two tissue compartment model (2TC) with an Efflux rate constant k_{loss} from the second tissue compartment (**Figure 1B**) was deemed to best represent the physiological processing of [¹¹C]5-HTP in the endocrine cell, including reversible uptake by LATs (K_1 and $k_2 > 0$) into the cytosol, irreversible enzymatic processing by DDC [¹¹C]5-HT or [¹¹C]serotonin ($k_3 > 0$ and $k_4 = 0$) and finally MOA-A mediated degradation and release of [¹¹C]5-HIAA into the blood stream (k_{loss}). In this model, the first tissue compartment would represent uncovered [¹¹C]5-HTP in the cytosol, while the second compartment would represent [¹¹C]serotonin in the cytosol or in vesicles. k_{loss} would represent direct release of [¹¹C]serotonin from the second compartment. The macro-parameter Flux or K_i was defined as $K_1 * k_3 / (k_2 + k_3)$. The vascular contribution (V_b) was set to 0.05 for all subjects.

IDIF derived from vena cava were used in all cases. The plasma-to-whole blood ratio was approximately 1 for all time-points, and regardless of pretreatment. Therefore, the plasma-to-whole blood ratio was kept constant at unity. The IDIF was corrected for metabolite stability, using population-based metabolite analysis for the different pretreatments (**Table 1**).

Statistical analysis

Differences between groups was assessed by a 2-tailed student's t-test using $\alpha = 0.95$.

Results

[¹¹C]5-HTP uptake in pancreas

As reported previously [11], but confirmed here with additional data, [¹¹C]5-HTP exhibited strong uptake in pancreas at baseline (**Figure 2**, top row). The retention in pancreas was higher than other abdominal tissues for up to 90 minutes, except the kidneys, which was due to urinary excretion. Pretreatment with DDC inhibitor carbidopa, which prevents the conversion of 5-HTP into serotonin, strongly reduced the retention in specifically the pancreas (**Figure 2**, middle row). Pretreatment with MOA-A inhibitors clorgyline, on the other hand, increased the retention of radioactivity in the pancreas, but not other abdominal tissues (**Figure 2**, bottom row).

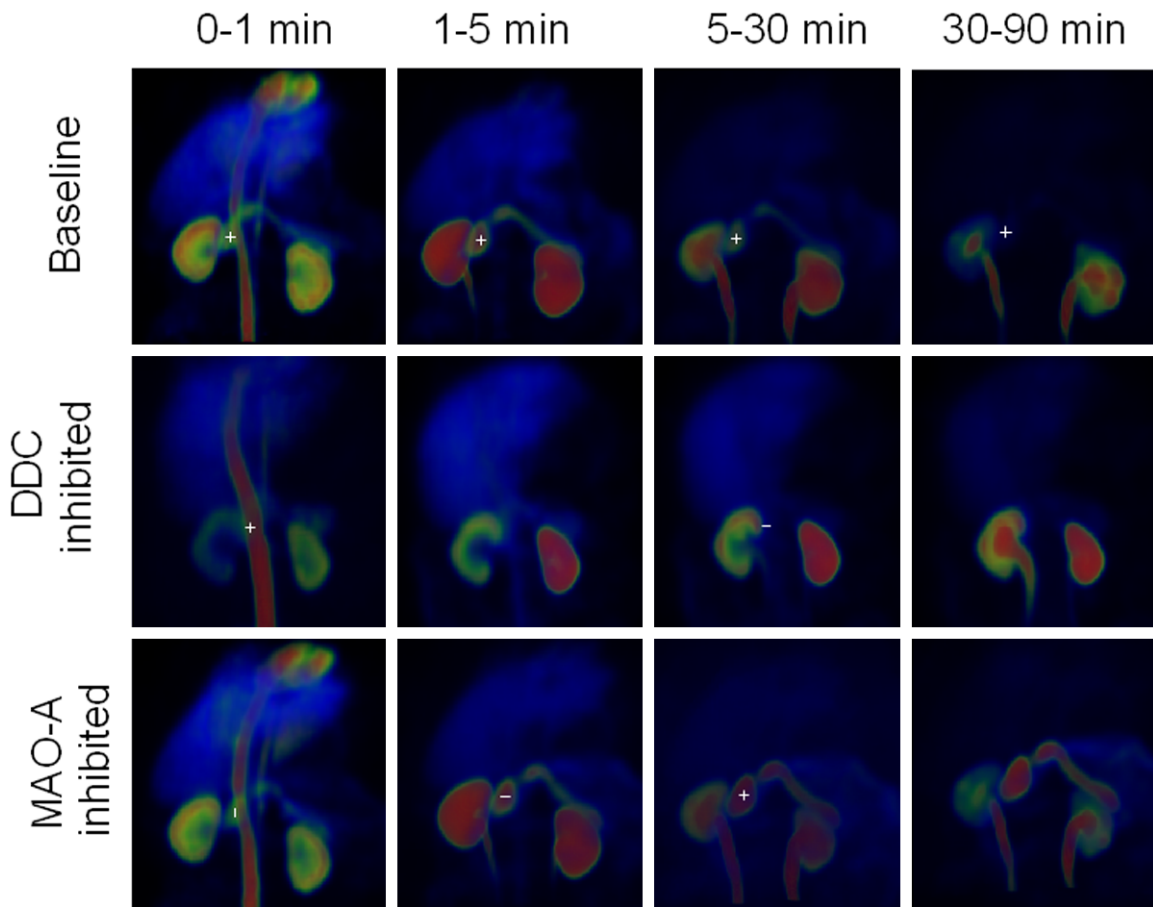


Figure 2. Maximum Intensity Projection (MIPs) visually showing the biodistribution and pancreatic uptake and retention of [^{14}C]5-HTP over time after injection. The biodistribution is shown at baseline conditions (top row), after pretreatment with DDC inhibitor Carbidopa (middle row) and after pretreatment with MAO-A inhibitor Clorgyline (bottom row). All images are normalized to SUV 15. The head of the pancreas is indicated by the white cross hairs.

The metabolic stability of [^{14}C]5-HTP was also impacted by pretreatment with carbidopa and clorgyline, where both compounds increased the percentage of intact [^{14}C]5-HTP at all time-points compared to baseline (**Table 1**).

Compartmental analysis

The time activity curves of [^{14}C]5-HTP exhibited distinctly different kinetics depending if scanned at baseline or following inhibition of DDC or MAO-A (**Figure 3**). At baseline, initial strong uptake in pancreas was followed by a slow efflux phase (**Figure 3A**). When inhibiting DDC, again initial uptake in pancreas was observed, but followed by very rapid washout from tissue (**Figure 3B**). Inhibition of MAO-A yielded high initial uptake in pancreas, similar as during baseline, but followed by a retention phase over almost 90 minutes (**Figure 3C**).

The 2TC k_{loss} model could describe all three modes of kinetics, despite the large variation seen in the uptake, washout and retention of [^{14}C]5-HTP (**Table 2**; **Figure 3A-C**).

Assessment of rate constants

K_1 was unchanged regardless of intervention (**Figure 4A**). Rate constant k_2 , i.e. the transport from the first tissue compartment to the blood compartment, was increased after pretreatment with carbidopa, but not clorgyline (**Figure 4B**). This agrees with the strong decrease seen for k_3 (the rate constant governing transport from the first to the second tissue compartment) after administration of carbidopa but not clorgyline (**Figure 4C**). Thus, by pharmacologically arresting the transport of [^{14}C]5-HTP in to the second tissue compartment forces an increase of k_2 instead.

Model of [¹¹C]5-HTP in pancreas

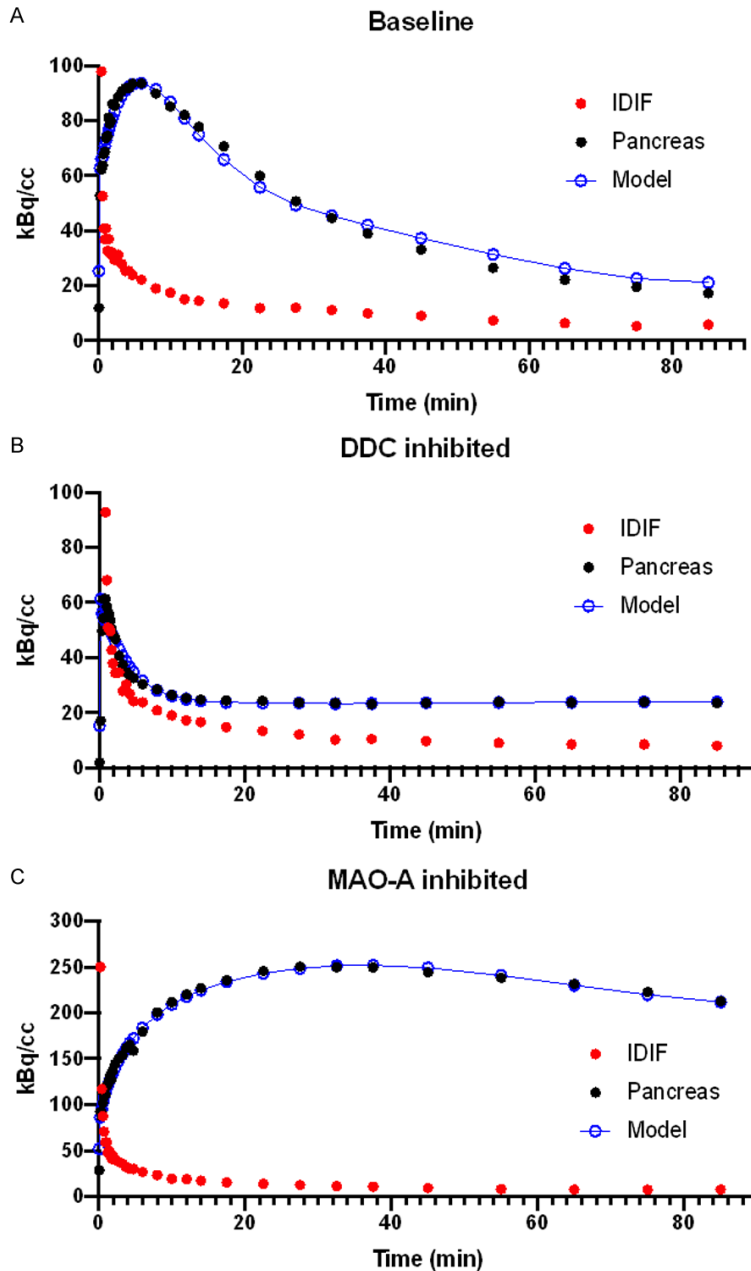


Figure 3. Representative examples of [¹¹C]5-HTP time activity curves (TACs) in pancreas at baseline (A), after pretreatment with carbidopa (B) or clorgyline (C). The TACs from pancreas and the IDIF (derived from vena cava) are indicated as black and red closed circles, respectively. The model fit is shown as blue line and open circles.

The efflux parameter k_{loss} was decreased both by pretreatment of carbidopa and clorgyline (**Figure 4D**). However, in the case of DDC inhibition by carbidopa, there is hardly any radioactivity in the second tissue compartment anyway, which presumably explains the decrease in k_{loss} , rather than a direct action of carbidopa

on k_{loss} . The clorgyline pretreatment, on the other hand, can be interpreted as a direct inhibition of the k_{loss} parameter.

Macro-parameters were also investigated, as they may provide improved robustness compared to individual rate constants, which may be overdetermined and not independent of each other. As expected from observing the changes in the individual rate constants, the Flux (K_1), was strongly decreased by carbidopa intervention (**Figure 4E**). The macro-parameter Flux/Efflux ratio (i.e. K_1 divided by K_{loss}) was strongly increased by MAO-A inhibition (**Figure 4F**).

Discussion

Here, we present a PET compartment model with sufficient complexity to describe multiple of the most important enzymatic steps in the processing and utilization of serotonin in neuroendocrine cells.

[¹¹C]5-HTP has been widely used as a general imaging marker of neuroendocrine tumors. Recently, [¹¹C]5-HTP has also been proposed as a marker for the endocrine pancreas in the context of islet mass and islet dysfunction in metabolic disease. Usually, semi-quantitative output such as SUV, SUV_{max} , %ID/g or %ID has usually been used from the PET scans for both appli-

cations. Although for example SUV may be an effective and robust endpoint, it is likely that that a static SUV value is an amalgam of several parallel processes, including uptake, wash-out and internal metabolism. Therefore, we propose that these processes can be disentangled by the selection of an appropriate compart-

Model of [¹¹C]5-HTP in pancreas

Table 2. Estimated rate constants, macro-constants and goodness-of-fit for all NHPs using the 2TC k_{loss} model

	K_1	k_2	k_3	k_{loss}	Flux (K_1)	Flux/Efflux (K_1/k_{loss})	Chi ²	R ²
Baseline	0.67	0	0.11	0.50	0.66	1.63	3.40	0.96
	0.85	0	0.18	0.73	0.85	1.17	2.29	0.96
	0.40	0	0.20	0.22	0.40	1.79	1.69	0.97
	0.51	0.02	0.13	0.36	0.45	1.24	4.16	0.95
	0.72	0.15	0.16	0.18	0.38	2.14	0.69	0.99
	0.74	0.18	0.14	0.09	0.31	3.38	0.65	0.99
	0.62	0.13	0.02	0.05	0.07	1.42	1.41	0.98
	1.93	0.33	0.38	0.17	1.03	5.89	0.25	1.0
	1.44	0.51	0.21	0.18	0.42	2.31	1.35	0.98
DDC inhibited	0.71	0.90	0.03	0.02	0.02	1.24	3.41	0.93
	0.56	0.54	0.007	0.01	0.007	0.54	7.15	0.94
	0.20	0.30	0.04	0.01	0.02	2.59	26.7	0.67
MAO-A inhibited	0.75	0.09	0.05	0.02	0.27	17.5	0.07	1.0
	0.46	0.03	0.01	0.003	0.15	43.9	0.14	1.0
	0.47	0	0.07	0.01	0.47	34.5	4.17	0.98
	0.58	0.04	0.07	0.02	0.38	20.0	0.36	0.99
	1.42	0.18	0.35	0.03	0.93	35.3	1.21	0.99

pancreas receives its tracer delivery from arterial blood. However, the cynomolgus animal model is quite small for the expected resolution of the Discovery ST PET/CT. Thus, there is a substantial risk for introducing variability due to partial volume effects when delineating a small tissue such as the descending aorta. The vena cava is easier to identify and accurately delineate, and was thus chosen as a proxy for the aorta. The descending aorta should be used as source for the IDIF in future analysis of human scans using this model, as the risk for partial volume effects is lower.

ment model and fitting of its rate constants to dynamic PET data of high temporal and spatial resolution of the pancreas.

The 2TC k_{loss} model (**Figure 1B**) is in theory similar to the generalized but widely accepted serotonin model of the neuroendocrine cell in **Figure 1A**. The standard 2TC model, on the other hand, lacks a rate constant describing direct efflux from the second tissue compartment. An alternative to the efflux rate constant would be to include the k_4 rate constant, describing flow of tracer from the second to the first tissue compartment - but this could also be interpreted as reconversion of [¹¹C]serotonin ([¹¹C]5-HT) back to [¹¹C]5-HTP, which in not a reasonable physiological or enzymatic process in the context of the neuroendocrine cell. A 3TC model including efflux from the second tissue compartment could in theory also incorporate the trapping of [¹¹C]5-HTP inside secretory vesicles (**Figure 1A**). However, such a model would include up to 5-6 parameters for fitting (K_1 , k_2 , k_3 , k_{loss} , k_5 , k_6), which likely would lead to over-determination of the equation system.

The vena cava was used as a source for the image derived image function (IDIF). This was a deliberate choice, despite the fact that the

The metabolic stability of [¹¹C]5-HTP varied depending on the intervention, to an extent that it should be taken into account when generating the IDIF. Since metabolic stability was not assessed in all NHPs, population based estimates were used. In the case of inhibition of DDC by carbidopa, data from only one NHP was available. In that animal, the metabolic stability of [¹¹C]5-HTP increased substantially. This is in line with a previous study in rhesus monkey, where 10 mg/kg of DDC inhibitor NSD1015 increased the metabolic stability of [¹¹C]5-HTP from approximately 50% to 85% at the 60 minute time-point [17]. Thus, it was deemed reasonable to extrapolate the stability data to all n=3 carbidopa treated NHPs in this study.

The 2TC k_{loss} model could adequately fit experimental data from pancreas from both from baseline scans (uptake and efflux), as well as from DDC inhibition scans (rapid washout) and MAO-A inhibition scans (strong retention). Importantly, the parameter estimation was relatively robust, enabling identification of which rate constant was affected by each of the interventions. In the case of carbidopa, the k_3 was decreased, which importantly could be inter-

Model of [¹¹C]5-HTP in pancreas

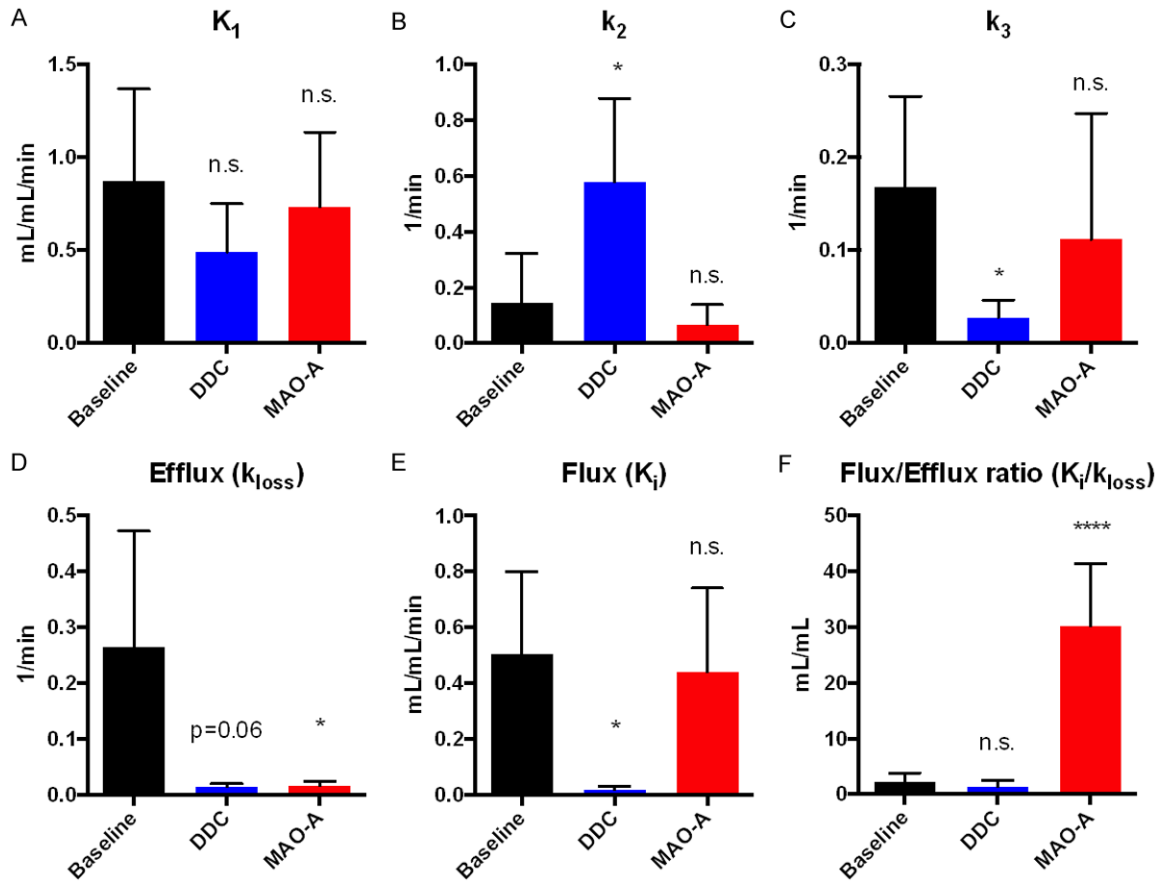


Figure 4. Estimated parameters of the 2TC model including efflux (k_{loss}) in pancreas at baseline (n=9) or following pretreatment with DDC inhibitor carbidopa (n=3) or MAO-A inhibitor clorgyline (n=5). The rate constants K_1 , k_2 , k_3 and k_{loss} (Efflux) are reported separately (A-D). The macro parameters Flux (or K_i) (E) and the Flux/Efflux ratio (F) may provide improved robustness.

preted as representing the enzymatic conversion of [¹¹C]5-HTP to [¹¹C]serotonin by DDC. Thus, the model confirms carbidopa as a DDC inhibitor. Clorgyline, on the other hand, affected primarily the Efflux parameter k_{loss} . Again, in the context of the model k_{loss} would represent the process of removing tracer from the second tissue compartment, i.e. MOA-A mediated conversion of [¹¹C]5-HTP into [¹¹C]5-HIAA and subsequent washout from the cell.

Some rate constants exhibited a substantial variability which is to be expected to some extent. Thus, macro-parameters such as the Flux (K_i) into the second tissue compartment as well as the Flux/Efflux ratio (K_i/k_{loss}) was even more robust in demonstrating the effect of the respective pharmacological interventions in the pancreatic serotonin metabolism.

Thus, the 2TC k_{loss} model accurately confirmed the known mechanisms of carbidopa and clor-

gyline on serotonergic processing in neuroendocrine tissue. The model can thus potentially be used for assessing changes in the different enzymatic steps in the pancreas in health and disease. This is of particular interest in the context of metabolic disease, where the molecular point of dysfunction can be pinpointed. For example, it is likely that destruction of islet mass in the pancreas would correspond to a decrease or loss of DDC enzymatic activity (since the acinar pancreas does not contain the molecular machinery for 5-HTP processing), and subsequently in a decrease of k_3 . However, recent publications have indicated that the loss of insulin secretion ability may be due to dedifferentiation of beta cells into neuroendocrine precursor cells, rather than outright beta cell destruction [14, 18-20]. Thus, accurate assessment of dysfunction at different points in the molecular machinery may assist in understanding the complex regulation and dysfunction of the endocrine pancreas in metabolic disease.

Conclusion

Here, we demonstrate a [¹⁴C]5-HTP compartmental analysis, which can quantitatively assess in vivo pharmacological interactions with several of the key steps of the serotonergic biosynthesis in pancreas. With this technique it is potentially possible to pin-point the origin of molecular function or dysfunction of the serotonergic metabolic pathway in the endocrine pancreas in health and disease.

Disclosure of conflict of interest

None.

Address correspondence to: Dr. Olof Eriksson, Science for Life Laboratory, Department of Medicinal Chemistry, Uppsala University, Dag Hammarskjölds väg 14C, 3tr, SE-752 37 Uppsala, Sweden. Tel: 0046-707903054; E-mail: olof.eriksson@ilk.uu.se

References

- [1] Kilbourn MR and Koeppe RA. Classics in neuroimaging: radioligands for the vesicular monoamine transporter 2. *ACS Chem Neurosci* 2019; 10: 25-29.
- [2] T L'Estrade E, Hansen HD, Erlandsson M, Ohlsson TG, Knudsen GM and Herth MM. Classics in neuroimaging: the serotonergic 2A receptor system-from discovery to modern molecular imaging. *ACS Chem Neurosci* 2018; 9: 1226-1229.
- [3] Narayanaswami V, Drake LR, Brooks AF, Meyer JH, Houle S, Kilbourn MR, Scott PJH, Vasdev N. Classics in neuroimaging: development of PET tracers for imaging monoamine oxidases. *ACS Chem Neurosci* 2019; 10: 1867-1871.
- [4] Ohta Y, Kosaka Y, Kishimoto N, Wang J, Smith SB, Honig G, Kim H, Gasa RM, Neubauer N, Liou A, Tecott LH, Deneris ES and German MS. Convergence of the insulin and serotonin programs in the pancreatic beta-cell. *Diabetes* 2011; 60: 3208-3216.
- [5] Paulmann N, Grohmann M, Voigt JP, Bert B, Vowinckel J, Bader M, Skelin M, Jevsek M, Fink H, Rupnik M and Walther DJ. Intracellular serotonin modulates insulin secretion from pancreatic beta-cells by protein serotonylation. *PLoS Biol* 2009; 7: e1000229.
- [6] Kim H, Toyofuku Y, Lynn FC, Chak E, Uchida T, Mizukami H, Fujitani Y, Kawamori R, Miyatsuka T, Kosaka Y, Yang K, Honig G, van der Hart M, Kishimoto N, Wang J, Yagihashi S, Tecott LH, Watada H and German MS. Serotonin regulates pancreatic beta cell mass during pregnancy. *Nat Med* 2010; 16: 804-808.
- [7] Ekholm R, Ericson LE and Lundquist I. Monoamines in the pancreatic islets of the mouse. Subcellular localization of 5-hydroxytryptamine by electron microscopic autoradiography. *Diabetologia* 1971; 7: 339-348.
- [8] Bird JL, Wright EE and Feldman JM. Pancreatic islets: a tissue rich in serotonin. *Diabetes* 1980; 29: 304-308.
- [9] Schraenen A, Lemaire K, de Faudeur G, Hendrickx N, Granvik M, Van Lommel L, Mallet J, Vodjdani G, Gilon P, Binart N, in't Veld P and Schuit F. Placental lactogens induce serotonin biosynthesis in a subset of mouse beta cells during pregnancy. *Diabetologia* 2010; 53: 2589-2599.
- [10] Ding WG, Fujimura M, Tooyama I and Kimura H. Phylogenetic study of serotonin-immunoreactive structures in the pancreas of various vertebrates. *Cell Tissue Res* 1991; 263: 237-243.
- [11] Eriksson O, Selvaraju R, Johansson L, Eriksson J, Sundin A, Antoni G, Sörensen J, Eriksson B and Korsgren O. Quantitative imaging of serotonergic biosynthesis and degradation in the endocrine pancreas. *J Nucl Med* 2014; 55: 460-5.
- [12] Eriksson O, Espes D, Selvaraju RK, Jansson E, Antoni G, Sörensen J, Lubberink M, Biglarnia AR, Eriksson JW, Sundin A, Ahlström H, Eriksson B, Johansson L, Carlsson PO and Korsgren O. Positron emission tomography ligand [¹⁴C]5-hydroxy-tryptophan can be used as a surrogate marker for the human endocrine pancreas. *Diabetes* 2014; 63: 3428-37.
- [13] Eriksson O, Selvaraju R, Eich T, Willny M, Brismar TB, Carlbom L, Ahlström H, Tufvesson G, Lundgren T and Korsgren O. Positron emission tomography to assess the outcome of intraportal islet transplantation. *Diabetes* 2016; 65: 2482-9.
- [14] Carlbom L, Espes D, Lubberink M, Martinell M, Johansson L, Ahlström H, Carlsson PO, Korsgren O and Eriksson O. [¹⁴C]5-hydroxy-tryptophan PET for assessment of islet mass during progression of Type 2 diabetes. *Diabetes* 2017; 66: 1286-1292.
- [15] Normandin MD, Petersen KF, Ding YS, Lin SF, Naik S, Fowles K, Skovronsky DM, Herold KC, McCarthy TJ, Calle RA, Carson RE, Treadway JL and Cline GW. In vivo imaging of endogenous pancreatic β -cell mass in healthy and type 1 diabetic subjects using 18F-fluoropropyl-dihydro-tetrabenazine and PET. *J Nucl Med* 2012; 53: 908-16.
- [16] Eriksson O, Laughlin M, Brom M, Nuutila P, Roden M, Hwa A, Bonadonna R and Gotthardt M. In vivo imaging of beta cells with radiotracers: state of the art, prospects and recommen-

Model of [¹⁴C]5-HTP in pancreas

- dations for development and use. *Diabetologia* 2016; 59: 1340-1349.
- [17] Lundquist P, Blomquist G, Hartvig P, Hagberg GE, Torstenson R, Hammarlund-Udenaes M and Långström B. Validation studies on the 5-hydroxy-L-[beta-¹¹C]-tryptophan/PET method for probing the decarboxylase step in serotonin synthesis. *Synapse* 2006; 59: 521-31.
- [18] Spijker HS, Song H, Ellenbroek JH, Roefs MM, Engelse MA, Bos E, Koster AJ, Rabelink TJ, Hansen BC, Clark A, Carlotti F and de Koning EJ. Loss of β -cell identity occurs in type 2 diabetes and is associated with islet amyloid deposits. *Diabetes* 2015; 64: 2928-38.
- [19] Wang YJ, Schug J, Won KJ, Liu C, Naji A, Avrahami D, Golson ML and Kaestner KH. Single-cell transcriptomics of the human endocrine pancreas. *Diabetes* 2016; 65: 3028-38.
- [20] Talchai C, Xuan S, Lin HV, Sussel L and Accili D. Pancreatic beta cell dedifferentiation as a mechanism of diabetic beta cell failure. *Cell* 2012; 150: 1223-34.